XXXVI Ibero-Latin American Congress on Computational Methods in Engineering
CILAMCE
Rio de Janeiro, 22-25 Nov 2015

DESIGN OF A WAVE-MAKER FACILITY THROUGH LINEAR WAVE THEORY

Rafael de Barros Passos

Antonio Carlos Fernandes

rbpassos@oceanica.ufrj.br

acfernandes@oceanica.ufrj.br

COPPE/UFRJ, Program of Ocean Engineering

Cidade Universitária - Centro de Tecnologia, CEP 21945-970, Rio de Janeiro, Brazil

Ramon Romankevicius Costa

ramon@coep.ufrj.br

COPPE/UFRJ, Program of Electrical Engineering

Cidade Universitária - Centro de Tecnologia, CEP 21945-970, Rio de Janeiro, Brazil

Abstract. *An important step in the development of new ocean structures is to conduct tests on reduced scale models in tanks that reproduce the environmental conditions of their operation. For the wave modeling in a 2D channel, waves are generated in one of its extremity by the wave-maker and should be absorbed at the far field by some beach. The present work analyses the linear wave theory applied to the wave-maker problem when a new wave-maker system is designed and implemented at LOC laboratory (COPPE/UFRJ). An experimental study is performed at the wave tank, generating regular time series and comparing the results with the predictions from linear wave theory.*

Keywords: *Wave-maker design, Linear wave theory, Servo-motor controller.*

1 INTRODUCTION

An important step in the development of new ocean structures is to conduct tests on reduced scale models in tanks that reproduce the environmental conditions of their operation. Recent advances in offshore industry have led to oil exploration increasingly in water depth, requiring laboratories all over the world to find an appropriated way of representing these new technical challenges with the precise accuracy.

For the wave modeling in a 2D channel, waves are generated in one of its extremity by the wave-maker and should be absorbed at the far field by some kind of beach. A tank equipped with a wave-maker is called a wave making basin from the perspective of ocean engineering. This article focus on the design and installation of a new wave-maker system to be assembled at LOC, Laboratory of Waves and Currents, at COPPE/UFRJ. Moreover, the proposed system is evaluated in the absorption mode, compounding the active wave absorber.

2 REVIEW OF THE HYDRODINAMIC WAVE-MAKER PROBLEM

The new wave-maker generation system will be of a flap type, powered by an electric engine. The actuation will be done by servo-motor, guided by a ball screw, connected to a rigid arm. Figure 1 shows a simplified model of a flap type wave-maker and the nomenclature used from now on.

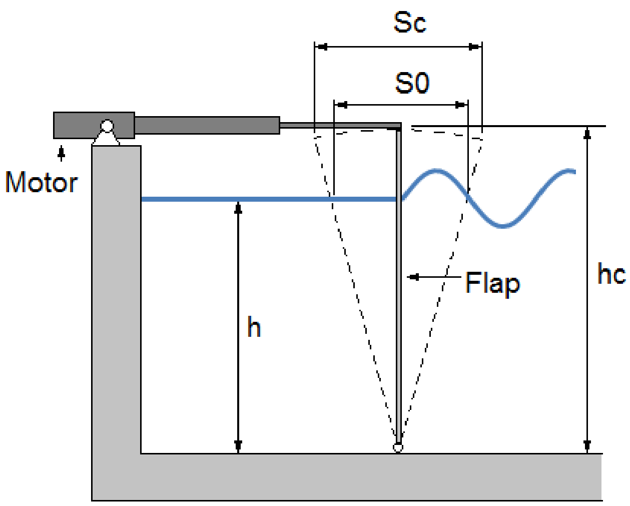

Figure 1 – Wave-maker model and nomenclature

The development of this problem follows the approach of a progressive wave propagating in an infinity domain (Dean and Dalrymple, 1991). The main difference is upon the boundary condition on the wave-maker wall ($x = 0$). In this boundary, considering small amplitudes for the wave-maker, the displacement profile can be described as a function of the depth z:

$$d(z) = \frac{S_0}{2}\left(1 + \frac{z}{h}\right) \tag{01}$$

Considering small amplitude of the oscillatory motion at the free surface level ($z = 0$), $\theta(t)$ is:

$$\theta(t) = \theta_0 Sen[\omega t] \cong \frac{S_0}{2h} Sen[\omega t] \qquad (02)$$

The condition that must be satisfied at boundary $x = 0$ is that fluid particles have the same normal velocity as the paddle. With that, the solution to the velocity potential can be written as:

$$\emptyset = A_0 \left(\frac{\omega}{k_0}\right) Cosh[k_0(z+h)] Exp[i(\omega t - k_0 x)] + \sum_{j=1}^{\infty} A_j \left(\frac{\omega}{k_j}\right) Cos\left[k_j(z+h)\right] Exp\left[i\left(\omega t - k_j x\right)\right] \qquad (03)$$

The first part of the potential represents the progressive waves, which propagates to infinity. The second part represents a series of stationary waves, usually called as evanescent modes. The amplitude of these evanescent waves decay exponentially with the distance from the wave-maker and its effect can be neglect at a distance of two to three times the water depth h. The wave number k_0 is related with the progressive mode as a solution of the dispersion equation:

$$\omega^2 = k_0 g Tanh[kh] \qquad (04)$$

On the other hand, the wave numbers k_j, which are related to the evanescent modes, are found as solutions of the trigonometric equation:

$$\omega^2 = -k_j g Tan[k_j h] \qquad (05)$$

After applying the condition at $x = 0$ the orthogonality between the cosine and hyperbolic cosine functions is applied to isolate the constants of the problem. The problem is defined obtaining the remaining coefficients bellow:

$$A_0 = \frac{i \int_{-h}^{0} d(z)\, Cosh[k_0(z+h)] dz}{\int_{-h}^{0} Cosh^2[k_0(z+h)]\, dz} \qquad (06)$$

$$A_j = -\frac{\int_{-h}^{0} d(z)\, Cos[k_j(z+h)] dz}{\int_{-h}^{0} Cos^2[k_j(z+h)]\, dz} \qquad (07)$$

The integration of the pressure field over the plate from the bottom ($z = -h$) to the free surface ($z = 0$) gives the horizontal force, F_x:

$$F_x = i\omega\rho\left(A_0\frac{\omega}{k_0}\int_{-h}^{0} Cosh\,[k_0(z+h)]dz + \sum_{j=1}^{\infty} A_j\frac{\omega}{k_j}\int_{-h}^{0} Cos\left[k_j(z+h)\right]dz\right)Exp[i\omega t] \quad (08)$$

Considering the rotational motion of a flap type wave-maker, the total moment with respect to the pivot point is then:

$$M_0 = i\omega\rho\left(A_0\frac{\omega}{k_0}\int_{-h}^{0} Cosh\,[k_0(z+h)](h+z)dz + \sum_{j=1}^{\infty} A_j\frac{\omega}{k_j}\int_{-h}^{0} Cos\left[k_j(z+h)\right](h+z)dz\right)Exp[i\omega t] \quad (09)$$

The equation of the rotational moment can be rewritten as a function of the angular speed, $\dot{\theta}(t)$, and the angular acceleration $\ddot{\theta}(t)$. The proportional parameters to these coefficients are the so called damping and added inertia of the structure, in the rotational motion.

Now this study can calculate the propagating incident wave height, far from the wave-maker. For that, only the progressive mode is necessary. Finally, it is possible to show that the correct transfer function to the wave-maker under design is the following (Frigaard and Andersen, 2010):

$$\frac{H}{S_0} = \frac{4Sinh[k_0h]}{k_0h}\frac{(k_0h\,Sinh[k_0h] - Cosh[k_0h] + 1)}{(Sinh[2k_0h] + 2k_0h)} \quad (10)$$

The graph of the proposed transfer function is obtained when the wave parameters are known. In Figure 2 the graph of this function is presented with the horizontal axis representing the wave frequency, although for naval architectures, sometimes the wave period appears to have a more physical meaning.

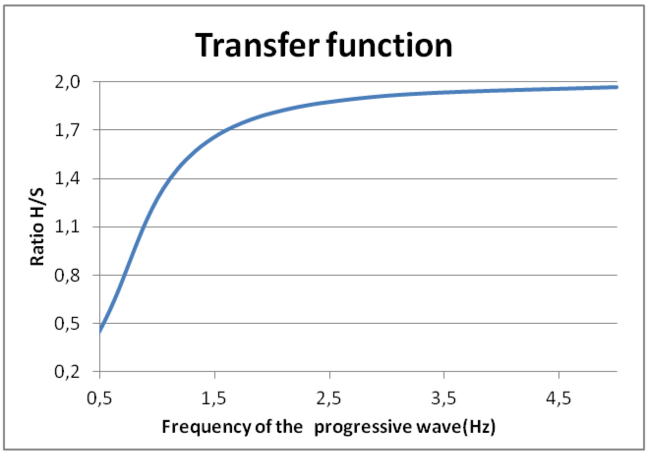

Figure 2 – Theoretical transfer function of the wave generation, H/S ratio

2.1 System capacity

In order to reproduce a wide range of wave periods at LOC wave channel, the new system will be analyzed between the following wave period (T_p) range: $0.5s \le T_p \le 2.5s$.

2.2 Maximum wave height and moments

To estimate the maximum wave height expected to each wave period one should attend the following requirements:

- Maximum steepness before wave breaking $\left(\frac{H}{L} < \frac{1}{7}\right)$;
- Maximum wave height that the physical limits of the water channel can admit ($H = 0.4$ to all wave periods, considering a water depth of $0.8m$);
- Maximum stroke of the actuator ($Sc = 0.5m$);
- Linear Acceleration limit of the actuator ($9.81m/s^2$);

To obtain maximum linear acceleration of the stroke, considering sinusoidal motions of the cursor which drives the flap, it is derived twice to find:

$$S(t) = \frac{Sc}{2} Sin[\omega t] \tag{11}$$

$$v(t) = \frac{Sc}{2} \omega Cos[\omega t] \tag{12}$$

$$a(t) = -\frac{Sc}{2} \omega^2 Sin[\omega t] \tag{13}$$

As the maximum admitted acceleration to the ball screw is established by the engine manufacturer as 1g ($9.81m/s^2$), the following condition must be respected to any wave period:

$$\frac{Sc}{2} \omega^2 \leq 9.81 \tag{14}$$

Figure 3 is composed by all the limitations above. Maximum wave height would be the area below to all the curves. The previous calculated transfer function must be used to linearly transfer all the conditions to the limit of the actuator stroke, at the connection point with the paddle plate.

Basically the wave breaking limit is the strictest condition until wave period of 1.2 seconds, and after that, the limitation is due to the maximum length of the piston ($0.5m$). After defining the maximum stroke at each period, the transfer function can be used again, now to find maximum wave height expected to each wave period, as presented in Figure 4.

According to Souza and Morishita (2003) the necessary total moment to drive the paddle plate is composed by the hydrodynamic reaction, the flap inertia and the weight moment of the plate. Considering now the rotational motion around the axis of the wave-maker, the calculated required moments are shown in Figure 5.

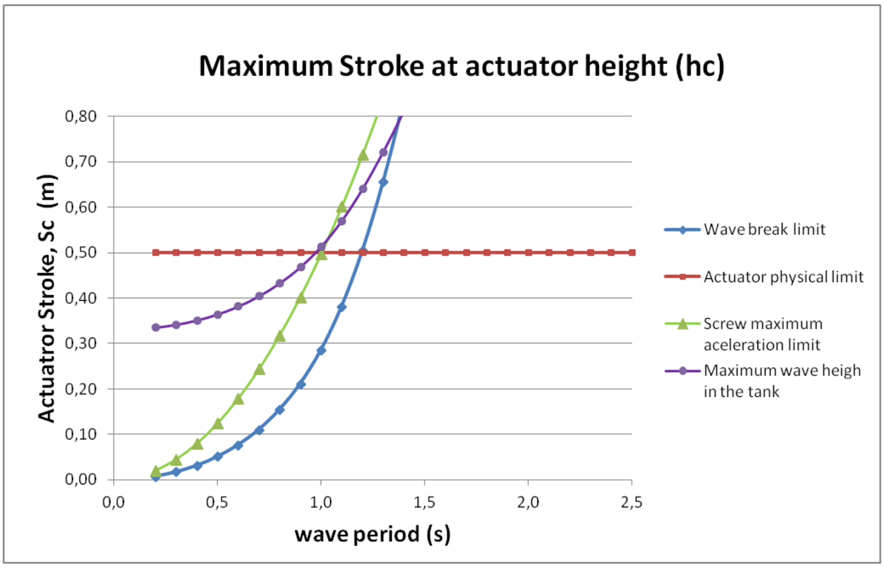

Figure 3 – Limitations of the wave-maker stroke

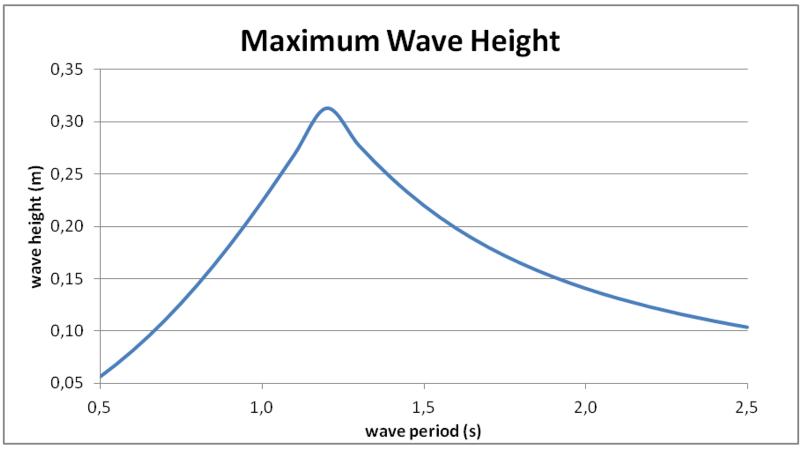

Figure 4 - Maximum wave height

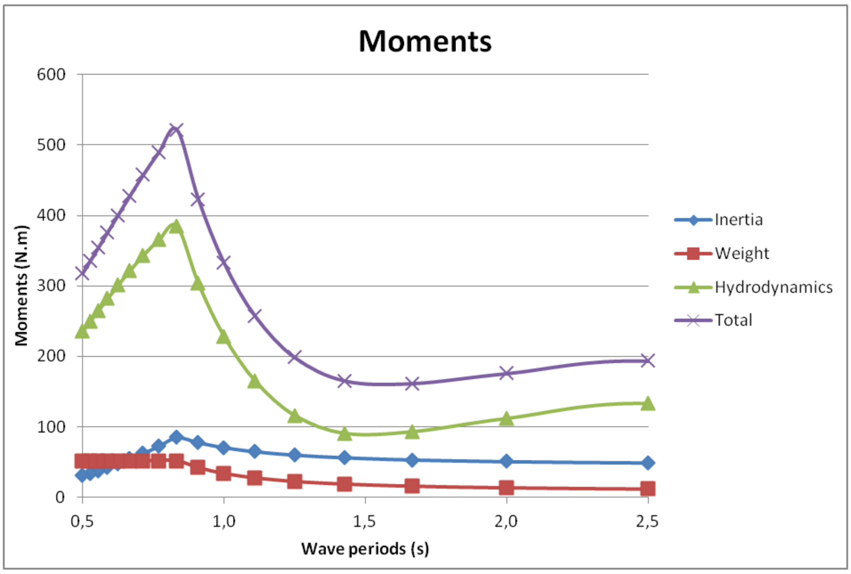

Figure 5 - Calculated total moments of the actuator

2.3 Hydrodynamics coefficients of the wave-maker

The methodology to determine the hydrodynamics coefficients (added mass and damping) for the wave-maker in an oscillatory motion was previously explained. Detailed description is performed by Passos *et. al.* (2015). Figure 6 and Figure 7 show these two coefficients as a function of the wave period of the generated wave over the wave channel.

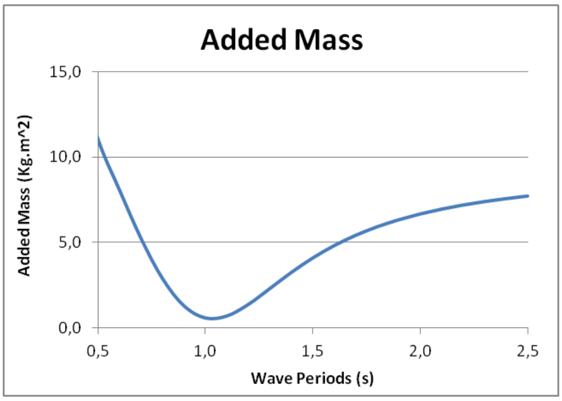

Figure 6 – Added mass hydrodynamic parameter

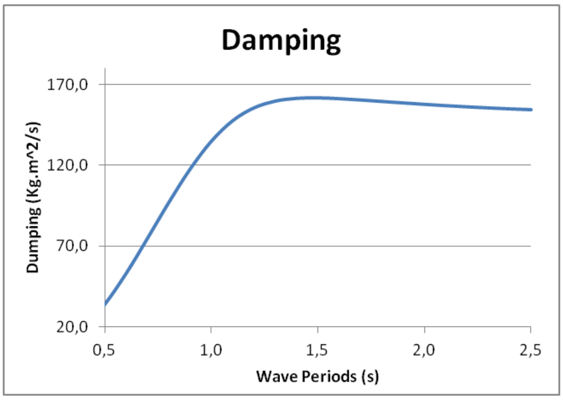

Figure 7 – Damping hydrodynamic parameter

3 CONTROL STRATEGY FOR THE WAVE-MAKER

This work used *feedfoward* and *feedback* controllers based on the second order dynamic problem of the rotational motion, since the added mass and damping coefficients were previously calculated through linear wave theory. Figure 8 shows a block diagram of the control system, designed for the new wave-maker. Figure 9 shows the final arrangement of this new electromechanical system installed at LOC wave channel. The computational tools necessary to develop the current work were built by means of the commercial software LabVIEW (2014).

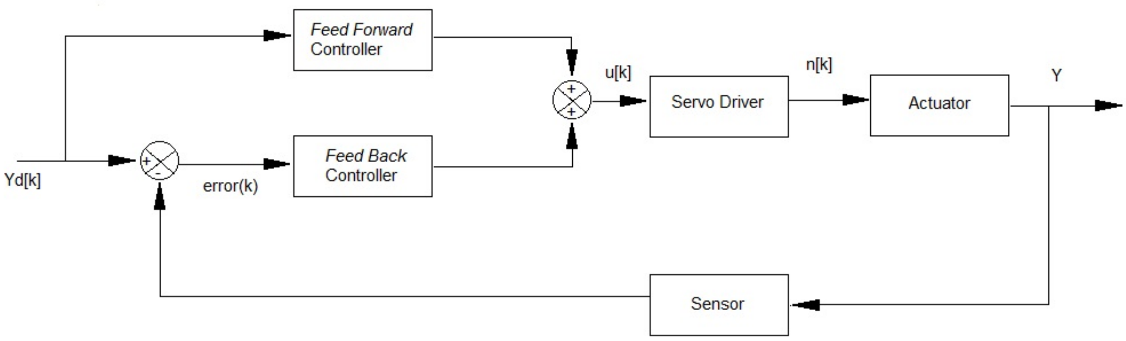

Figure 8 – Block diagram of the control system of the wave-maker

Figure 9 – Final arrangement at LOC wave channel

3.1 Experimental analyses

The experimental arrangement along LOC wave channel is presented in Figure 10. Good agreement with the sinusoidal function was obtained, especially to the small amplitude waves. The experiments were conducted using a passive beach in the opposite end of the channel, to absorb the waves generated by the new wave-maker, getting longer duration for the time series under analysis. The wave period and amplitudes were calculated by peak statistical analyses in the permanent state of each time series record.

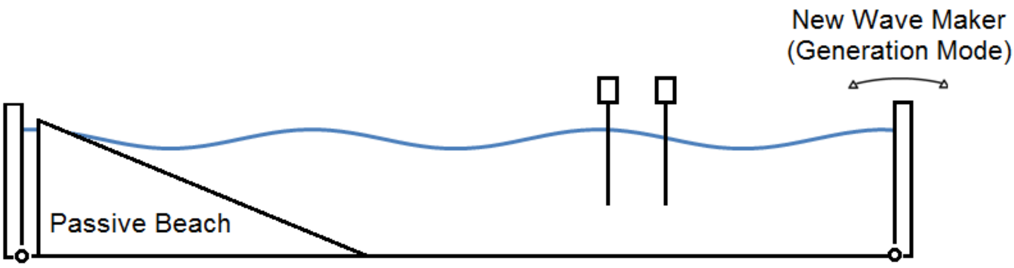

Figure 10 – Wave generation along the 2D wave channel

In order to validate the predictions of wave height by linear wave theory the research generated small amplitude waves with steepness less than 0.02. The wave steepness is the ratio between wave height and wave length and is a non-dimensional parameter. A comparison between linear wave theory and the experimental analyses is presented in Figure 11 and the relative errors are presented in Figure 12. It must be noted that the theoretical linear prediction are the same as presented in Figure 2 but the horizontal axis is now representing the wave periods, in seconds.

The data analysis found that better fit is obtained to long waves, which here means larger periods. For the small period waves, since the wave length is extremely reduced, the amplitude became so small that the signal-noisy ration became relevant. In the perspective of the linear wave theory, which assumes infinity long waves, the results show good agreement between theory and experiments, with less than 10% difference to almost all of the tested waves.

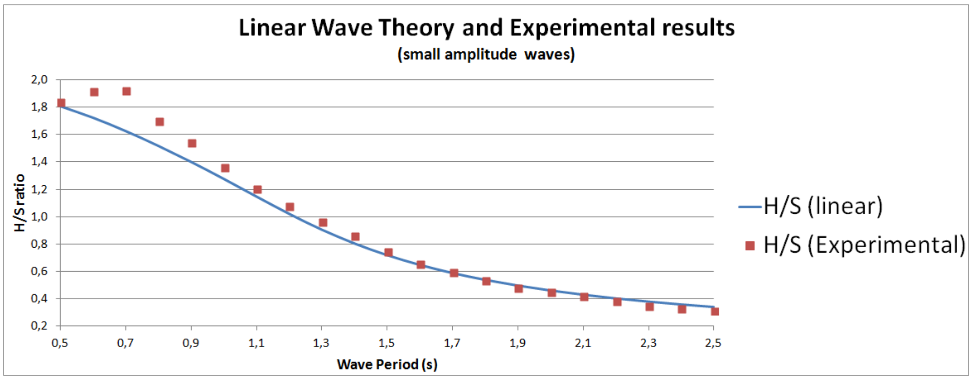

Figure 11 – Comparison between linear wave theory and experimental analysis

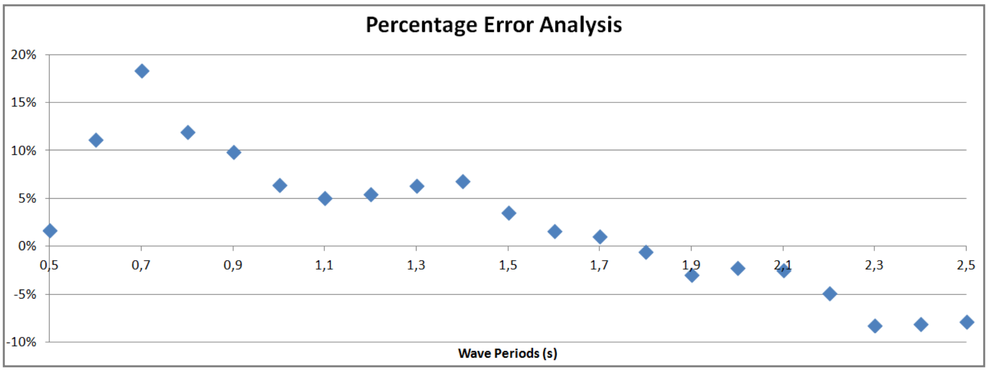

Figure 12 – Percentage error of the previous comparison

After validating the wave generation mode, the study performed some tests to investigate the use of this wave-maker as an active wave absorber. LOC laboratory provides an additional wave-maker system to generate waves, while the proposed new system was tested in the absorption mode.

To achieve the objective of active absorption, the tests made use of wave-probes sensors located far from the paddle, to measure the wave height and period. From these parameters, and assuming linear wave theory, the motion of the actuator is controlled by the incident wave to be absorbed. Figure 13 shows the laboratory arrangement to perform tests with the active wave absorber simultaneously with a wave-generation system.

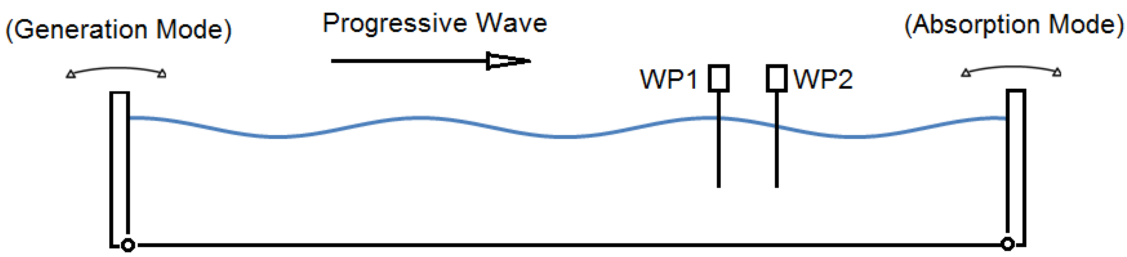

Figure 13 - Wave absorption along the 2D wave channel

Figure 14 and Figure 15 show a sequence of shots at specific positions of the actuator during the absorption tests. It is clear that the wave profile seems to have continuity from both sides of the plate. The active wave absorber works indeed as a transparent wall. In Figure 16 the incident and reflected time series are presented together, after an on-line separation, using the actual time series from both wave-probes (Frigaard, 1995).

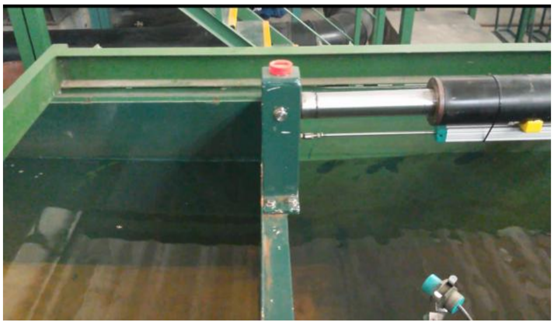

Figure 14 – Actuator near the through position of a 1.0 second wave period

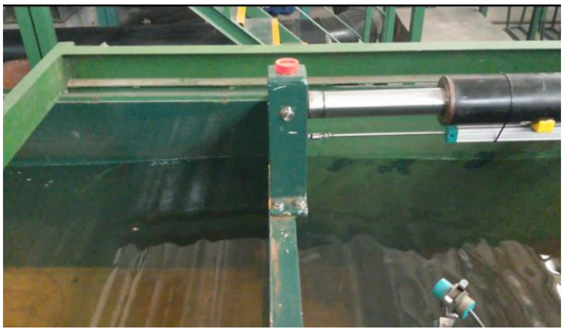

Figure 15 - Actuator near the peak position of a 1.0 second wave period

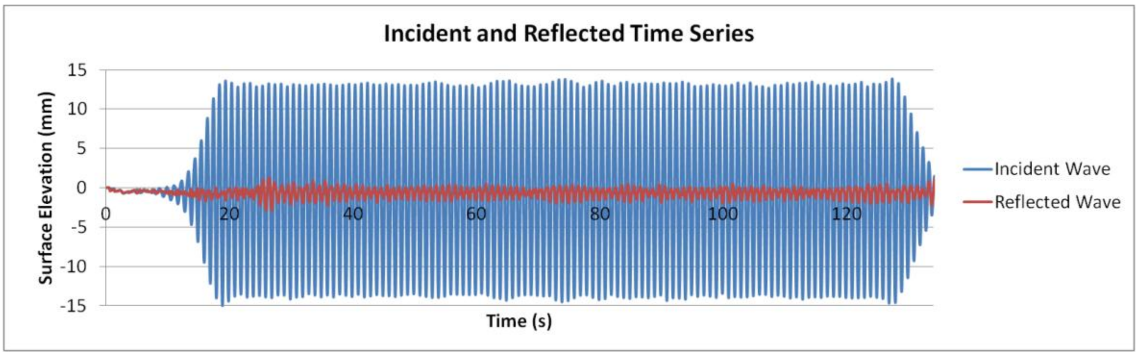

Figure 16 - Incident and Reflected time series measured at WP1 position.

The calculated value for the reflection coefficient found for the presented wave (1.0 second wave period) was Cr = 4.91%. This absorption level is comparable with those calculated with the passive beach feature (Mello, 2006).

4 CONCLUSIONS AND FUTURE WORKS

This work presented some steps to design a new wave-maker system, essential for reduced scale model tests, mainly applied to the offshore industry. The system was initially tested with small steepness waves, generated in the 2D wave channel, at LOC laboratory (COPPE/UFRJ).

Results show good agreement between linear wave theory predictions and experimental waves generated by the new system. The control architecture was designed exclusively to the present work and discrete implemented with the plant by commercial software LabVIEW.

In addition, good absorption level was obtained when the system was tested in the absorption mode, using both wave-makers available at the laboratory. Future works could include the validation of the same system when the random waves are to be absorbed by the active beach.

ACKNOWLEDGEMENTS

Thanks for all support provided by KeppelFels during the period of this research. In addition, be grateful to BrasFels Shipyard for the construction of the paddle plate used as the flap wave-maker.

REFERENCES

Dean, R. G. and Dalrymple, R. A., 1991. Water wave mechanics for engineers and scientists. Singapore: World Scientific.

Frigaard, P., & Andersen, T. L., 2010. Technical Background Material for the Wave Generation Software. Aalborg: Department of Civil Engineering, Aalborg University , DCE Technical Reports; No. 64.

Frigaard, P., & Brorsen, M., 1995. A time-domain method for separating incident and reflected irregular waves. Coastal Engineering 24 , 205-2015.

Mello, P. C., 2006. Um aparato para redução de reflexão de ondas em praia parabólica. *Master Dissertation-COPPE/PENO*

Passos, R. B. *et. al.*, 2015. Design and construction of an active wave absorber in a wave channel. To be published by COPPE/UFRJ. M.Sc. dissertation. Rio de Janeiro.

Souza, C. A. and Morishita, H. M., 2003. Evaluation of a flap type wave generator. 17th Int.Cong. of Mechanical Engineering.